Incorporating Rubble Mound Jetties in Elliptic Harbor Wave Models

Vijay Panchang[1]; Jianfeng Zhang[2]; and Zeki Demirbilek[3]

Abstract: Simulation models based on the elliptic mild- or steep-slope wave equation are frequently used to estimate wave properties needed for harbor engineering calculations. To enhance the practical applicability of such models, a method is developed to accommodate the effects of rubble mound structures that are frequently found along the sides of harbor entrance channels. The results of this method are found to match those of other mathematical models under appropriate conditions but also to deviate from those of parabolic approximations in some cases as a consequence of increased angular scattering induced by dissipation. Comparison with hydraulic model data also shows that this approach is useful for designing pocket wave absorbers that are used to attenuate wave heights in entrance channels.

DOI: 10.1061/(ASCE)0733-950X(2008)134:1(40)

CE Database subject headings: Wave propagation; Jetties; Harbors; Numerical models; Simulation models.

Introduction

In projects involving the design or modification of harbors, engineers frequently use computational models based on the 2D elliptic mild-slope wave equation to estimate the desired wave properties. This equation is intended to reproduce simultaneously the effects of refraction, diffraction, and reflection (induced by structures as well as bathymetric variations) in domains of arbitrary shape for the entire range of practical wave conditions. The equation has also been extended to include wave-current interaction (Chen et al. 2005), wave breaking (Zhao et al. 2001), floating docks (Li et al. 2005), and steep-slope effects (Chandrasekara and Cheung 1997). Sophisticated numerical models have therefore been developed in recent years and used in many practical harbor problems. These include studies of Ste. Therese de Gaspe Harbor, Kahului Harbor, Morro Bay Harbor, Venice Lagoon, Los Angeles/Long Beach Harbor, and Barbers Point Harbor (Tang et al. 1999; Okihiro and Guza 1996; Thompson and Demirbilek 2002; Thompson et al. 2002; Panchang and Demirbilek 2001; Mattioli 1996; Kostense et al. 1988; Bova et al. 2000; Zubier et al. 2003).

One problem frequently encountered by engineers using such models pertains to the presence of rubble-mound structures in the modeling domain. For instance, many harbor entrance channels have rubble-mound jetties along their sides. The jetties serve to prevent cross-channel sediment transport when they project out into the ocean and to prevent erosion along the channel sides when the channel is bounded by land. When properly designed, they are also intended, in part, to attenuate wave conditions that could adversely impact navigation (Melo and Guza 1991a,b). In some cases, however, provision of a rubble-mound structure along the channel sides is not possible because it infringes on the navigable waterway. Alternative methods of wave attenuation must then be considered. One alternative method consists of building local expansions in the waterway in which rubble mound may be placed. (The remainder of the channel side may be much smoother than the rubble mound boundary). Configurations like these have been referred to as "pocket wave absorbers" by Thompson et al. (2004, 2006); however, comparable localized channel expansions, which can also be built in rivers (near bridge abutments), have been more generally referred to as "side porous caves" by Sulisz (2005).

Many configurations for the pocket absorbers are possible (Fig. 1), and wave heights in the channel are influenced by the shape, length, and location of the rubble mound sections. In some

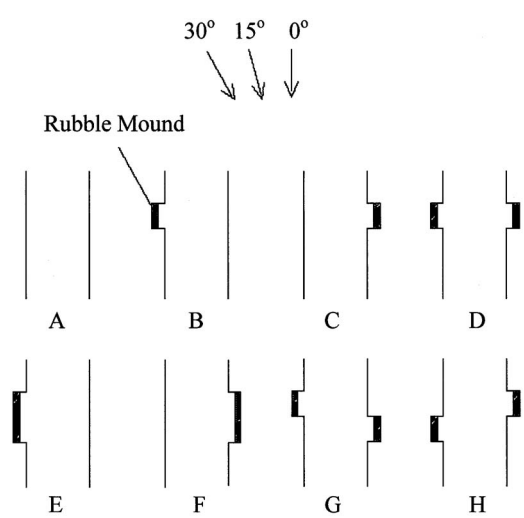

Fig. 1. Pocket absorber configurations

[1]Department of Maritime Systems Engineering, Texas A&M Univ., 200 Seawolf Parkway, Galveston, TX 77553 (corresponding author). E-mail: panchanv@tamug.edu

[2]Department of Maritime Systems Engineering, Texas A&M Univ., 200 Seawolf Parkway, Galveston, TX 77553.

[3]U.S. Army Engineer R&D Center, Coastal and Hydraulics Laboratory, Vicksburg, MS 39180-6199.

Note. Discussion open until June 1, 2008. Separate discussions must be submitted for individual papers. To extend the closing date by one month, a written request must be filed with the ASCE Managing Editor. The manuscript for this paper was submitted for review and possible publication on August 2, 2006; approved on January 29, 2007. This paper is part of the ***Journal of Waterway, Port, Coastal, and Ocean Engineering***, Vol. 134, No. 1, January 1, 2008. ©ASCE, ISSN 0733-950X/2008/1-40–52/$25.00.

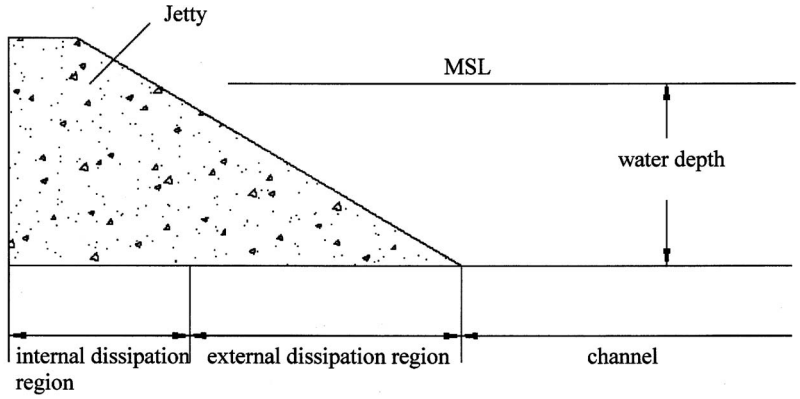

Fig. 2. Definition sketch for jetty modeling

cases, waves can be reflected off the absorbers, creating larger waves on the up-wave side of the pockets (Sulisz 2005) that can be hazardous to small craft operation. Proper estimation of the rubble mound's effect on the wave properties is therefore important in obtaining optimum designs. However, the absence of methodologies for designing pocket wave absorbers was noted as an impediment by Thompson et al. (2004) when they performed engineering work for entrance channels in the Great Lakes region.

In the context of the mild-slope wave model that is frequently used for harbor wave modeling, pioneering efforts were made by Melo and Guza (1991a,b) to incorporate the dissipation associated with rubble mound jetties. They parameterized this nonlinear phenomenon with "internal" and "external" friction formulations to describe the dissipative processes within the jetty pores and over the jetty slope, respectively. The actual formulations were described via the Lorentz principle. To solve the model equations, however, they resorted to the parabolic approximation Melo and Guza (1991a,b). In this approach, solutions from the previous finite-difference row can be used to estimate the nonlinear terms necessary to march the solution to the next row in an iterative fashion. Unfortunately, this forward-marching approach compromises solution accuracy in cases of reflections, such as those described by Sulisz (2005) in the vicinity of pocket wave absorbers and by Melo and Gobbi (1998) in the vicinity of curved channels. Further, multiple models may have to be used for complex geometries, which is inconvenient. In their study of wave propagation in the Mission Bay entrance channel, for instance, Melo and Gobbi (1998) had to use two parabolic approximation models: one based on Cartesian coordinates for the straight part and one based on polar coordinates for the curved part, with the output from one model providing the input to the other. This approach, besides being cumbersome, relies on the "assumption that the back-reflected wave field at the junction is negligible" (Melo and Gobbi 1998).

More recently, Sulisz (2005) developed a model based on the solution of the 3D Laplace equation. Boundary conditions near the rubble-mound jetty were described by the porosity and appropriate damping coefficients. The solution was based on subdividing the model domain into several subdomains of constant depth and solving the Laplace equation on each via the boundary-element method with appropriate matching at the interfaces. Although there are no limitations pertaining to wave reflections or scattering in this method, the solution of the wave propagation problem in the entire harbor by the boundary element method is not viable because this approach leads to full matrices that are prohibitively large for short waves.

Both methods described above (i.e., the parabolic approximation model and the 3D Laplace equation model) can therefore be applied only to selected portions of an overall harbor domain. Elliptic mild-slope wave models, on the other hand, can be used to perform simulations on the entire domain. Resulting from advances in iterative solution methods, in finite element grid generators, and in graphical user interfaces (see Panchang and Demirbilek [2001] for a review), robust codes are now available that can be efficiently applied to large domains of complex shape. Well-known models used by engineers include PHAROS, CGWAVE, and EMS. The purpose of this paper is to explore the incorporation of the dissipative effects of rubble-mound jetties in such models, thus extending their capabilities for practical engineering applications. The paper may be regarded as a continuation of the efforts described by four papers published in recent years in this journal.

Methodology

Several investigators (e.g., Booij 1981; Dalrymple et al. 1984; Tsay et al. 1989) have proposed that frictional effects can be

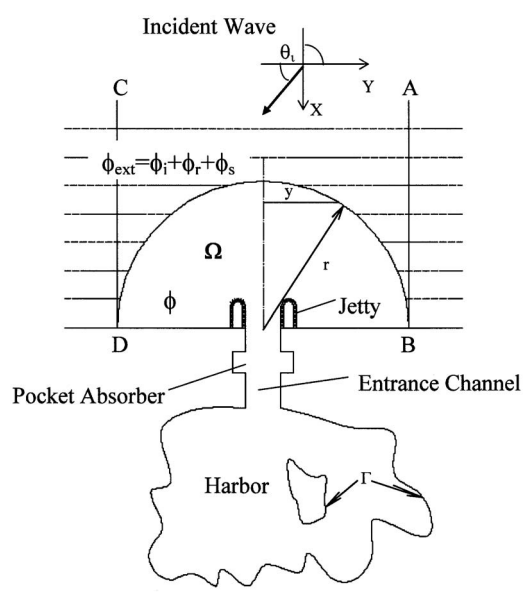

Fig. 3. Harbor wave model domain, definition sketch

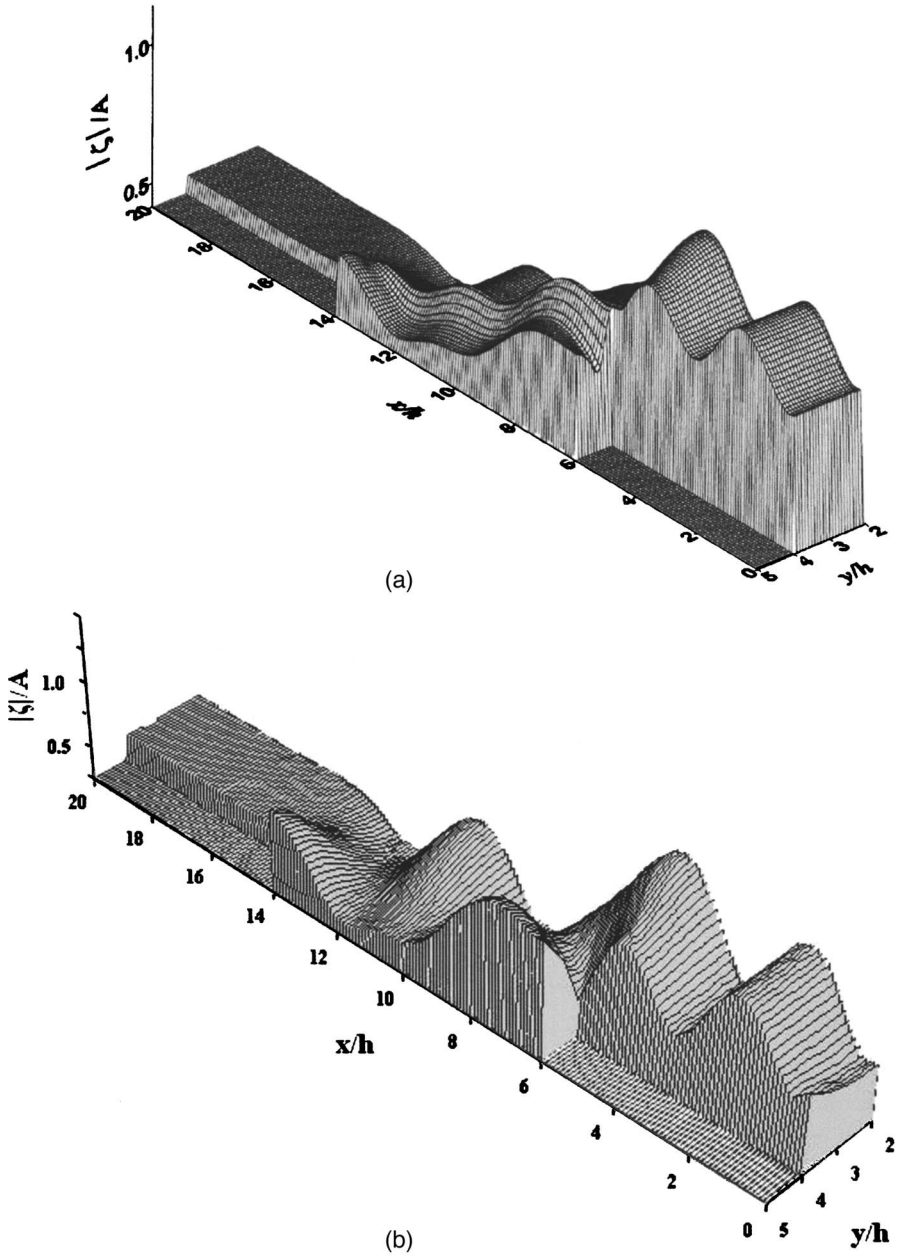

Fig. 4. Wave amplitude comparison in a channel 2 pocket wave absorbers: (a) 3D model (Sulisz 2005); (b) present elliptic model

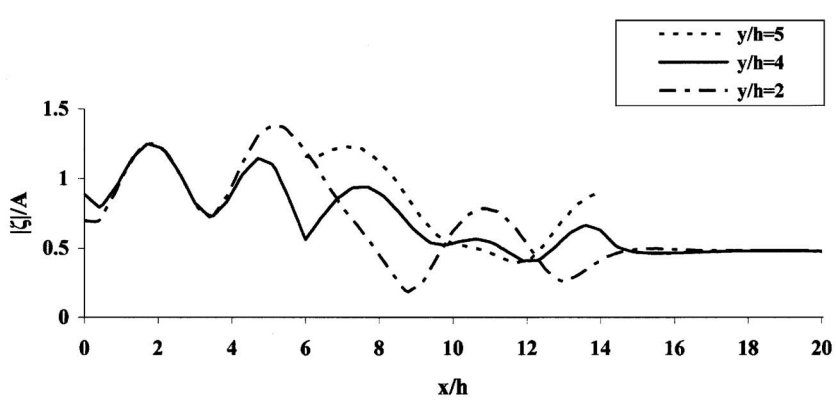

Fig. 5. Modeled (normalized) wave amplitudes

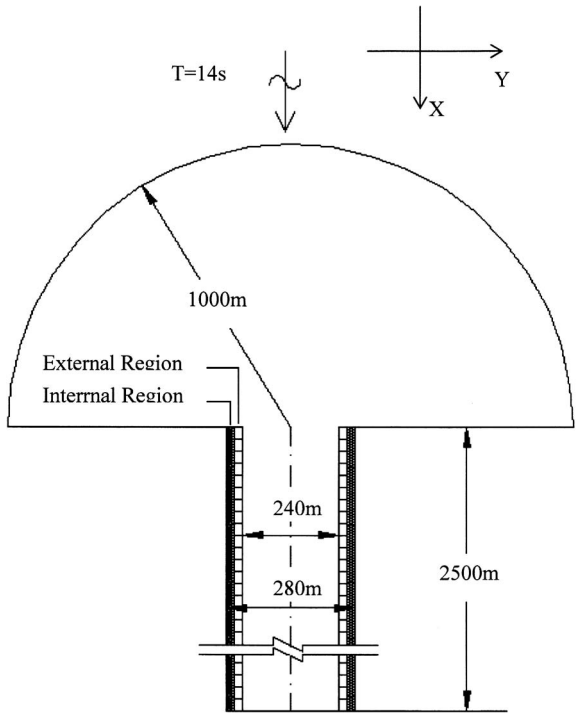

Fig. 6. Straight channel model domain (after Melo and Guza 1991a)

introduced in the mild-slope equation in the form of a parameterized dissipation term as follows:

$$\nabla \cdot (CC_g \nabla \phi) + (CC_g k^2 + i\sigma w)\phi = 0 \tag{1}$$

where $\phi(x,y)=\phi_1+i\phi_2$=complex surface elevation function, from which the wave height can be obtained; $i=\sqrt{-1}$; σ=wave frequency under consideration; $C(x,y)$=phase velocity; $C_g(x,y)$ =group velocity; w=friction factor; $k(x,y)$=wave number, related to the local depth $h(x,y)$ through the wave dispersion relation.

Dalrymple et al. (1984) and Tsay et al. (1989) have summarized several parameterized forms for the friction factor w. These include the effects of a porous bottom, a viscous mud bottom, a laminar bottom boundary layer, a densely packed surface film, and natural vegetation (seaweed, trees, etc). Their formulations do not appear to be directly applicable to the dissipative effects of rubble-mound jetties; Melo and Guza (1991a) have therefore used a parameterization based on the Lorentz principle. They recommend subdividing the jetty cross section into two areas: the submerged portion is described as an "external" dissipation region, and the part further away from the water is described as an "internal" dissipation region (Fig. 2). Dissipation coefficients, f_{ext} and f_{int}, are then assigned to each region; these may be related to the original friction factor w as follows:

$$w = fkC_g, \quad \text{where } f = f_{int} \text{ or } f_{ext} \tag{2}$$

The external dissipation coefficient f_{ext} depends on the wave energy dissipated per unit area over a rough, steep slope. Since this is difficult to estimate, Melo and Guza (1991a) have related it to a local reflection coefficient (R) in a simple manner

$$f_{ext} = \frac{1-R^2}{kD_e} \tag{3}$$

where D_e= width of the external dissipation region of the model jetty. When R is specified by the user, f_{ext} is easy to estimate. In contrast, the estimation of f_{int} is more complicated. After formulating the dissipation in the pores as a combination of laminar and turbulent stresses ($=\alpha q+\beta|q|q$, where q represents flux), Melo and Guza (1991a) and Sulisz (2005) have invoked the Lorentz principle of equivalent work to relate f_{int} to α and β:

$$f_{int} = \frac{1}{\sigma}(\alpha + \beta\lambda_q) \tag{4}$$

In Eq. (4), λ_q=a function of the velocity through an elemental pore volume and may be estimated, following the derivation of Melo and Gobbi (1990), as

$$\lambda_q = \frac{8}{3\pi}\left|\frac{-igk}{\sigma(S-if_{int})}\right||A^*(x,y)| \tag{5}$$

where $|A^*(x,y)|$=a characteristic mean wave amplitude within a small representative pore volume; and S=inertia coefficient with a nominal value ~1. For the laminar and turbulent stress coefficients α and β used in Eq. (4), Melo and Guza (1991a) suggest the following descriptions (based on previous research):

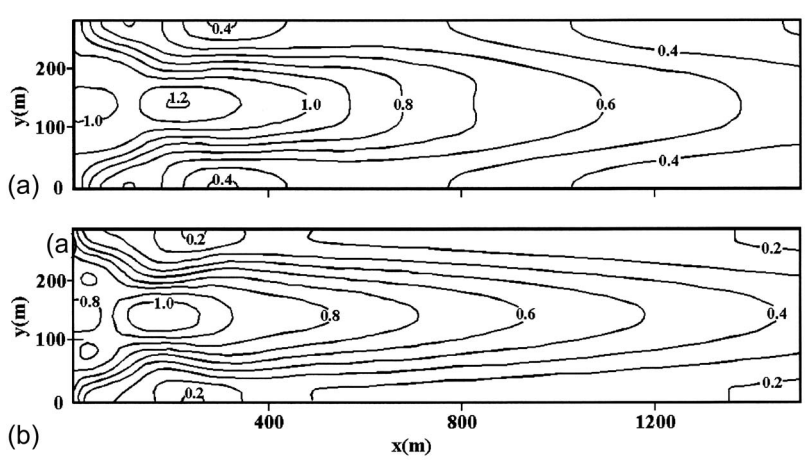

Fig. 7. Wave height comparison for $\theta=0°$: (a) parabolic approximation (Melo and Guza 1991a); (b) present elliptic model

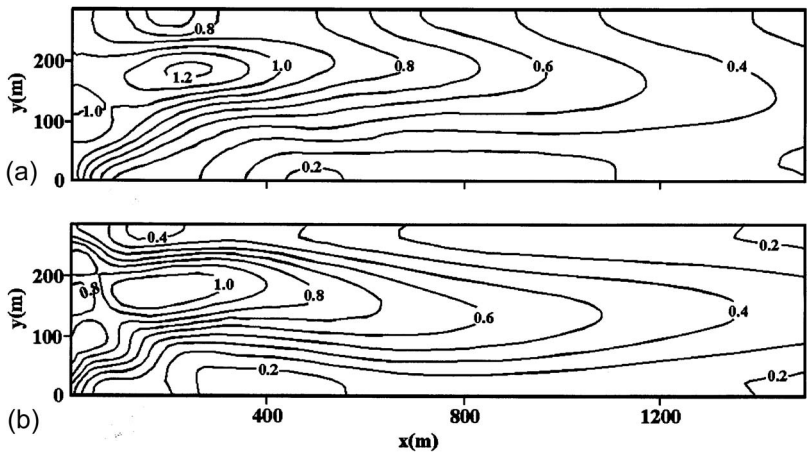

Fig. 8. Wave height comparison for $\theta = 10°$: (a) parabolic approximation (Melo and Guza 1991a); (b) present elliptic model

$$\alpha = \alpha_0 \frac{(1-n)^3}{n} \frac{v}{d^2} \beta = \beta_0 \frac{(1-n)}{n} \frac{1}{d} \tag{6}$$

where n=porosity (ratio of void to total volume) for rubble-mound structures; v=kinematic viscosity of water; d=rock diameter; and α_0 and β_0=constants with average values of 1,000 and 2.7, respectively. The resulting parameterization for f_{int} is a function of the wave properties and renders the model nonlinear.

When w is known, the solution of the elliptic Eq. (1) can be obtained for any domain of arbitrary shape (Tsay et al. 1989; Demirbilek and Panchang 1998). Boundary conditions along coastlines and other closed boundaries (denoted by Γ in Fig. 3) can be written in terms of the normal derivative and a user-specified reflection coefficient. Along the open boundary (denoted by the semicircle in Fig. 3), the potential ϕ consists of three components: the incident wave (ϕ_i) that must be specified to

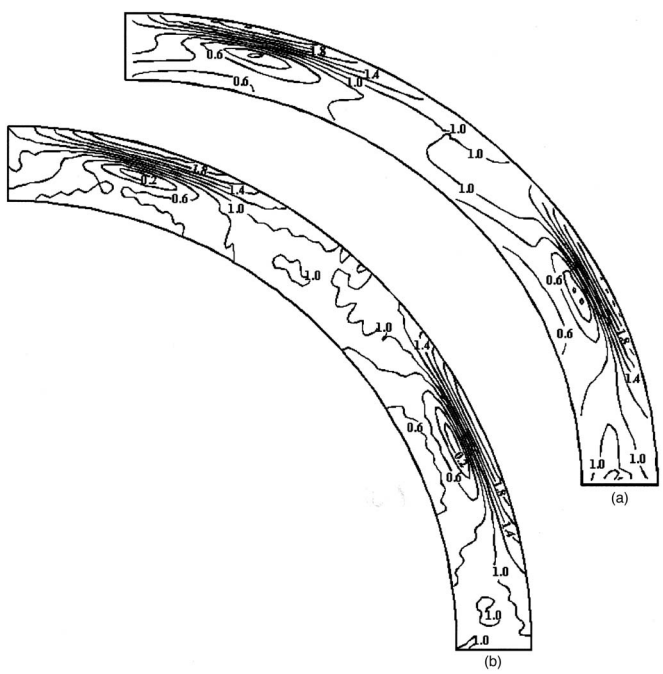

Fig. 9. Wave height comparison in narrow circular channel, no dissipation: (a) parabolic approximation (Melo and Gobbi 1998); (b) present elliptic model

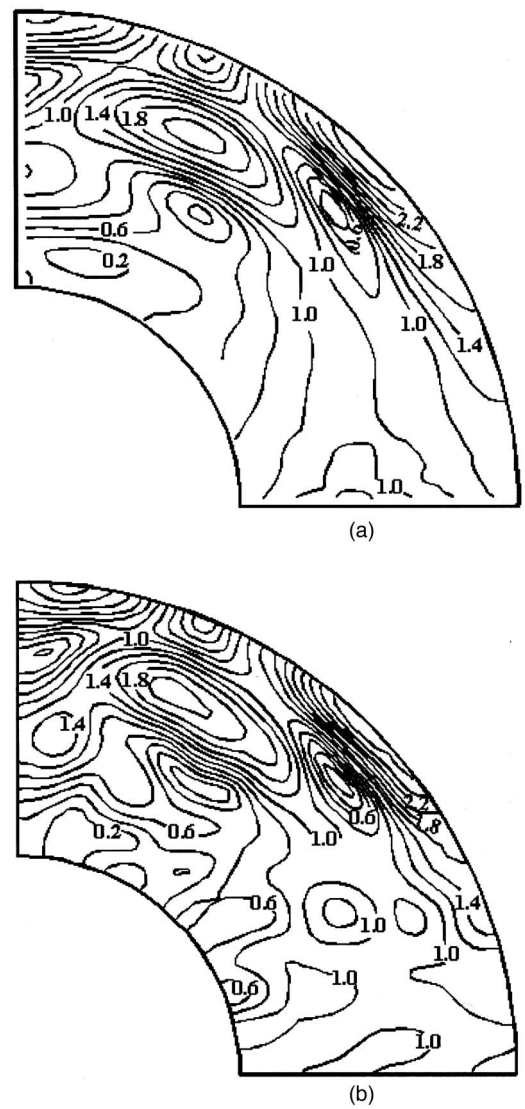

Fig. 10. Wave height comparison in wide circular channel, no dissipation: (a) parabolic approximation (Melo and Gobbi 1998); (b) present elliptic model

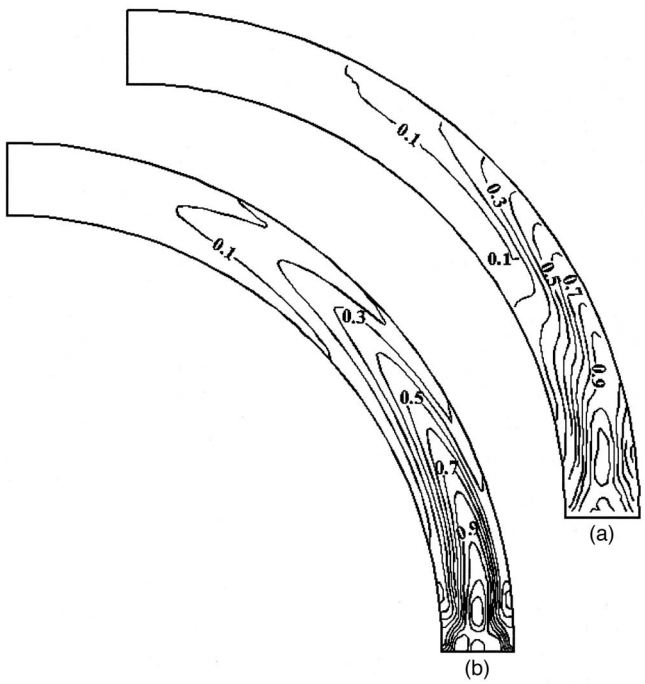

Fig. 11. Wave height comparison in narrow circular channel, with dissipation: (a) parabolic approximation (Melo and Gobbi 1998); (b) present elliptic model

force the model, a reflected wave (ϕ_r) that would exist in the absence of the harbor, and a scattered wave (ϕ_s) that emanates as a consequence of the harbor. With appropriate descriptions for these components, a boundary condition can be developed along the semicircle. The procedure can be summarized as follows: The exterior region is represented by two 1D transects denoted by AB and CD (with depths varying in the cross-shore direction only), and the incident wave is specified at the offshore end. A 1D version of Eq. (1) is used to solve for the combination of ϕ_i and ϕ_r (denoted by ϕ_o) along the transects. Then ϕ_o is laterally transposed onto the semicircle. Introducing $\phi_s = \phi - \phi_o$ into an appropriate radiation equation for the scattered wave completes the treatment of the open boundary condition. Mathematical details of these boundaries conditions are provided in Panchang et al. (2000) and Panchang and Demirbilek (2001). One may avail of the finite element method for a numerical solution (Demirbilek and Panchang 1998). A typical harbor model grid contains about 250,000 nodes (depending on the harbor dimensions and the desired resolution of L/10), and a solution can be obtained using conjugate gradients (Li 1994; Panchang et al. 1991; Bova et al. 2000).

Since the dissipation factor w (or, more specifically, f_{int}) is a function of the wave amplitude [according to Eqs. (4) and (5)] and is unknown a priori, Eq. (1) must be solved by iteration. For the first iteration, w is set equal to 0 (i.e., linear [frictionless] solutions are obtained). The resulting wave heights are used to estimate w, and Eq. (1) is solved again. The process is repeated until the solutions converge. Issues pertaining to the convergence are comparable to those discussed in detail by Zhao et al. (2001) in the context of wave breaking.

Validation against Other Mathematical Solutions

The model described above was first tested against solutions obtained by other methods for two test cases. (Several other elementary cases, such as wave propagation over regions with two friction values (Dalrymple et al. 1984), were also simulated to test the code.) The first case consists of wave propagation in a rectangular channel with two pocket wave absorbers (configuration D in Fig. 1). The geometry consists of a channel of depth 1 m and width 4 m along which two rectangular pocket absorbers of length 8 m (along the channel) and width 1 m are placed. An incident wave of amplitude 0.5 m and period 2.3 s was specified for the simulation. Rubble mound placed in the pocket absorber was described by $f_{int}=0.25$ and $f_{ext}=0$; no stone was placed along the other boundaries, which were treated as fully reflective. The solution of the elliptic Eq. (1) is compared in Fig. 4 to that obtained by Sulisz (2005) using the 3D Laplace equation. (Fig. 4 shows only half the domain for reasons of symmetry.) The results are largely the same. There are some differences between the two solutions, but they are minor and may be attributed to the different methods used to parameterize the dissipation term in the 2D and 3D models. Both solutions show cross modes in the channel near the pocket absorbers, increased wave heights on the up-wave side of the pocket wave absorbers, and wave attenuation on the down-wave side. Based on Fig. 5, which depicts modeled wave heights along three transects, reflections on the up-wave side can be as high as 40%.

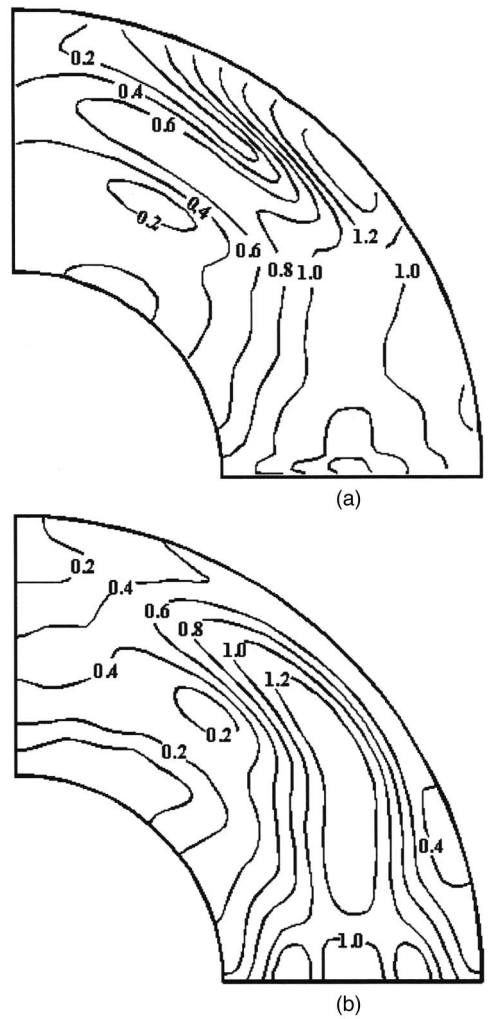

Fig. 12. Wave height comparison in wide circular channel, with dissipation: (a) parabolic approximation (Melo and Gobbi 1998); (b) present elliptic model

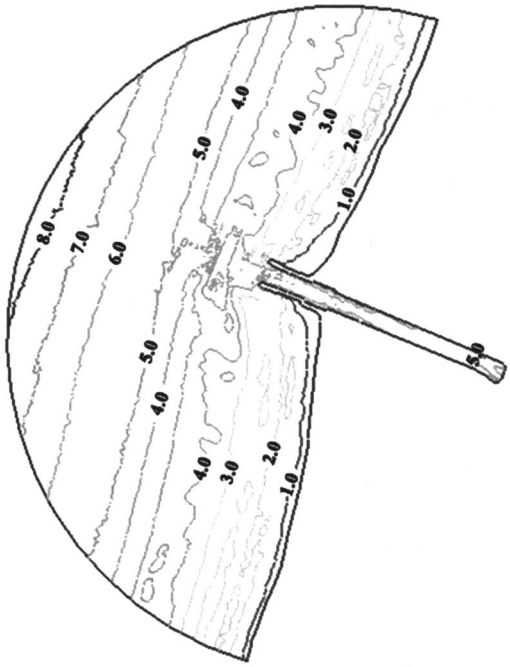

Fig. 13. Pentwater Harbor entrance channel model (depth in m)

The second test consists of wave propagation in a straight channel bounded laterally by rubble mound jetties (Fig. 6). The jetty parameters are $n=0.45$; $d=1.25$ m; and $f_{ext}=0.5$, and the input wave has an amplitude of 0.4 m and period 14 s. A solution to this problem was obtained previously by Melo and Guza (1991a) using parabolic approximations accurate to different orders. The elliptic equation model domain used here consisted of the rectangular region connected to a semicircular external area of radius 1000 m and contained 97,761 triangular elements. The solution converged to a (normalized) tolerance of the order of 10^{-6} after about 19 iterations. The elliptic model solutions are compared against the results of Melo and Guza (1991a) in Figs. 7 and 8 for incident wave angles=0° and 10°. The salient features of the two sets of results are similar.

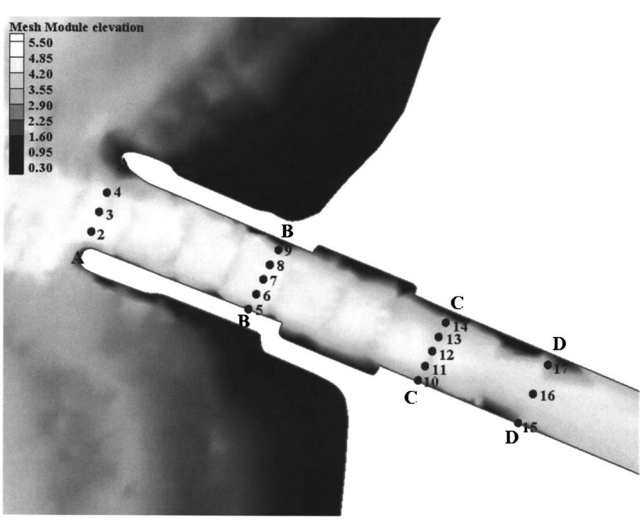

Fig. 14. Pentwater entrance channel, hydraulic model gauge locations (numbered dots), and bathymetry (in m)

The similarity of the present (2D elliptic model) solutions with other solutions, one that is in principle a more complete model (the 3D Laplace model) and the other an approximation of the present model (the 2D parabolic approximation) inspires faith in the reliability of the present model. In the following section, therefore, we explore additional cases in comparison with the present case and develop solutions to them.

Other Simulations

We first consider the case of wave propagation in circular (or curved) channels with jettied side walls as an extension of the straight channel case described above. Solutions to this problem have been obtained by Melo and Gobbi (1998) using a parabolic approximation in polar coordinates. Two cases with different radii of curvature were examined. To study the jetty wall's effects on the solutions, Melo and Gobbi performed simulations with and without the stone rubble along the walls (i.e., with and without w). The results from the present elliptic model are compared against those of Melo and Gobbi (1998) in Figs. 9–12. Figs. 9 and 10 (the no-friction case) suggest that the discrepancies between the results of the parabolic approximation and those of the full elliptic model solution are fairly small. This is somewhat surprising, in view of the limitations of the parabolic models concerning the direction of wave scattering. The differences are much greater when the dissipative effects of the jetties are introduced (Figs. 11 and 12). The wave height contours resulting from the elliptic model appear to be shifted toward the inside of the curve relative to those resulting from the parabolic model. Since the parabolic approximation can accommodate wave scattering in a limited aperture, one can infer that the enhanced wave scattering induced by the jetties is an impediment to the approximate model. The elliptic model has no such restrictions and therefore its results shown in Figs. 11 and 12 may be used as the benchmark solutions for future modeling studies. Also, considerably smaller wave heights result as a consequence of the rubble mound sides (Figs. 9–12).

We next examine the performance of the model in a nonidealized situation. To mitigate navigation problems, pocket wave absorbers have been constructed in the entrance channel leading to Lake Michigan near Pentwater Harbor (Thompson et al. 2004, 2006). A physical model study performed at the U.S. Army Engineer Coastal and Hydraulics Laboratory provides some data for model validation. Figs. 13 and 14 show the model bathymetry, which is patterned after the Pentwater Harbor geometry. In this case, rubble mound structures are present seaward of the coastline as well as in the pocket absorbers. For numerical simulation, a model domain containing 161,862 nodes was constructed. All side boundaries were specified as fully reflecting and the down-wave boundary as fully absorbing. To demonstrate the effects of the jetty, we performed simulations with and without friction for normally incident waves of height 1 m and period 5 s. (Fig. 15). It can be seen that the channel geometry (without dissipation) creates large waves (shown in blue) in some areas in the channel, in particular, along the south jetty, along the north pocket, and along the north wall down-wave of the pocket absorber (Fig. 15, top panel). The dissipative effects of the rubble mound causes attenuation of these large waves; also, the overall wave heights on the down-wave side of the pocket absorber are somewhat smaller (more red, less green) when dissipation is invoked. A similar reduction in wave heights is seen outside of the north jetty also.

Wave height measurements were made by Thompson et al. (2006) along four transects (AA, BB, CC, DD) using gauges

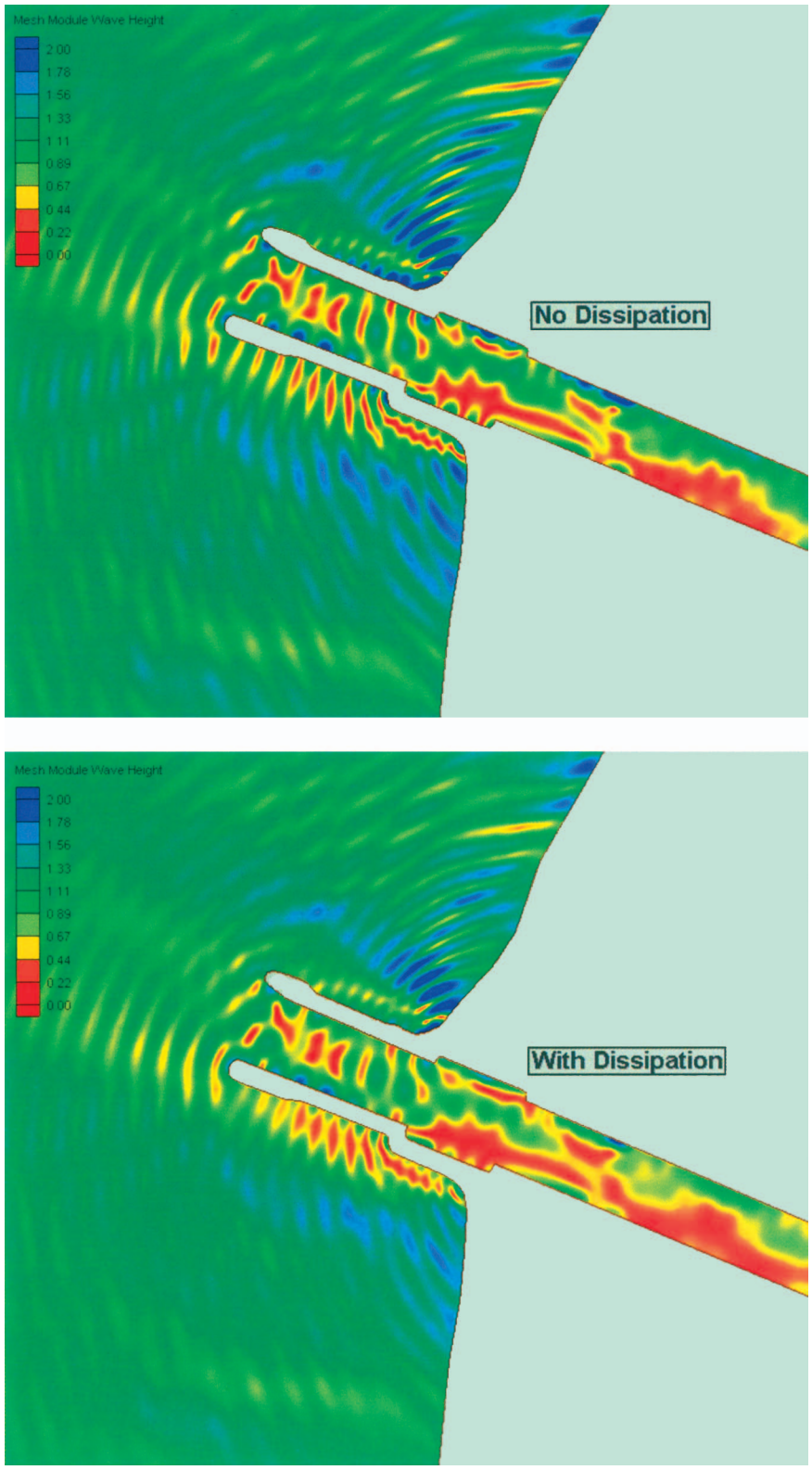

Fig. 15. (Color) Modeled wave height comparison

denoted by circular dots numbered 2 through 17 in Fig. 14. Although the wave-maker generated spectral (unidirectional) waves, examination of some of the hydraulic model photographs (e.g., Figs. 16 and 17) suggested that a monochromatic representation was perhaps acceptable for efficiency of numerical simulation for our purpose. In any case, full details of the incident wave spectrum were not readily available. Simulations for the following cases were performed: (a) incident wave height $H_i=1$ m, $T=5$ s; (b) $H_i=2$ m, $T=8$ s, and (c) $H_i=2$ m, $T=7$ s. Also, incident wave angles of 0° and 45° were considered.

Numerical simulations and hydraulic model photographs are shown for cases (a) and (b) in Figs. 16 and 17, for incident wave

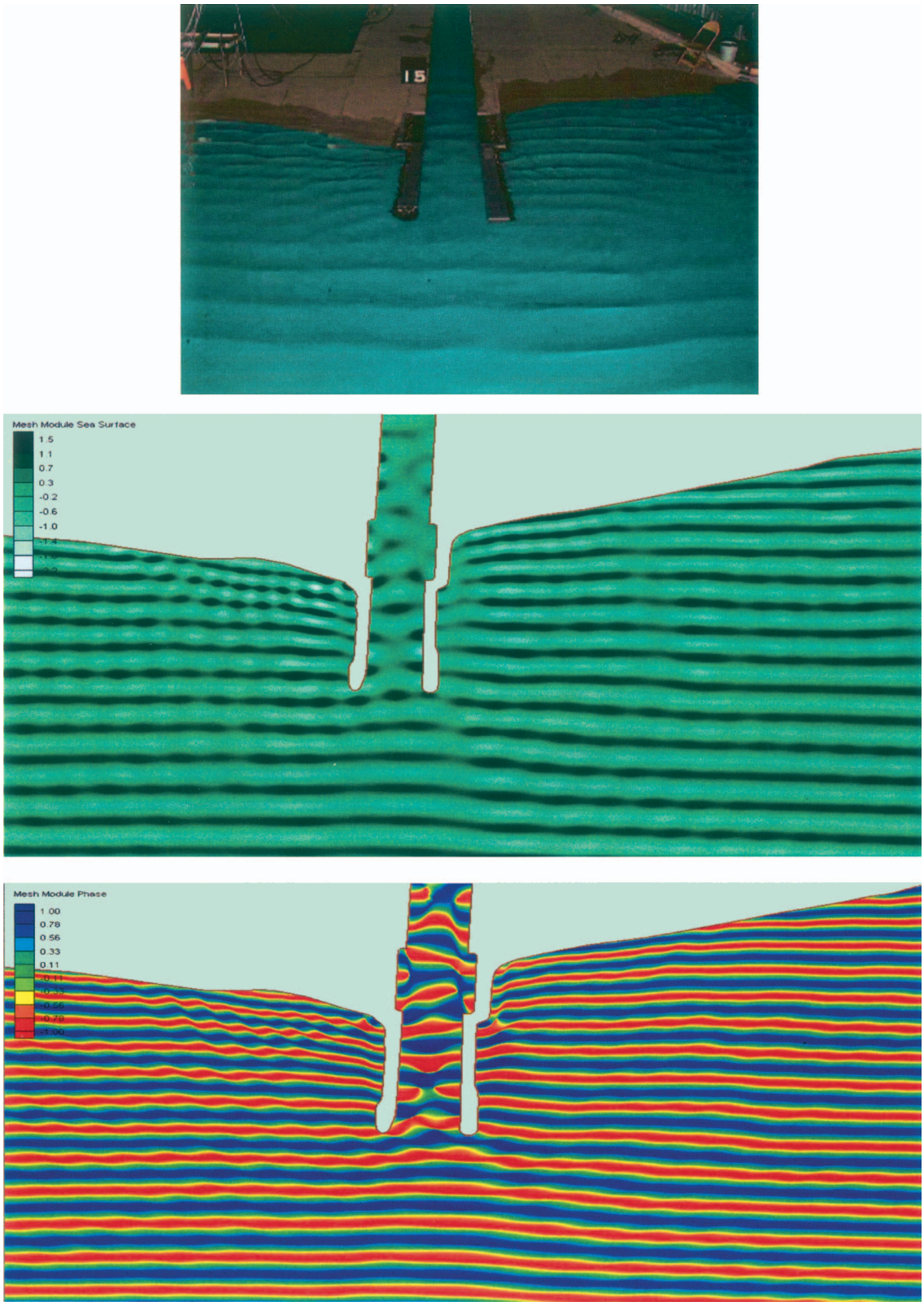

Fig. 16. (Color) Hydraulic and numerical model sea surface snapshot (top two panels) and numerical model phase diagram (bottom panel) for normally incident wave

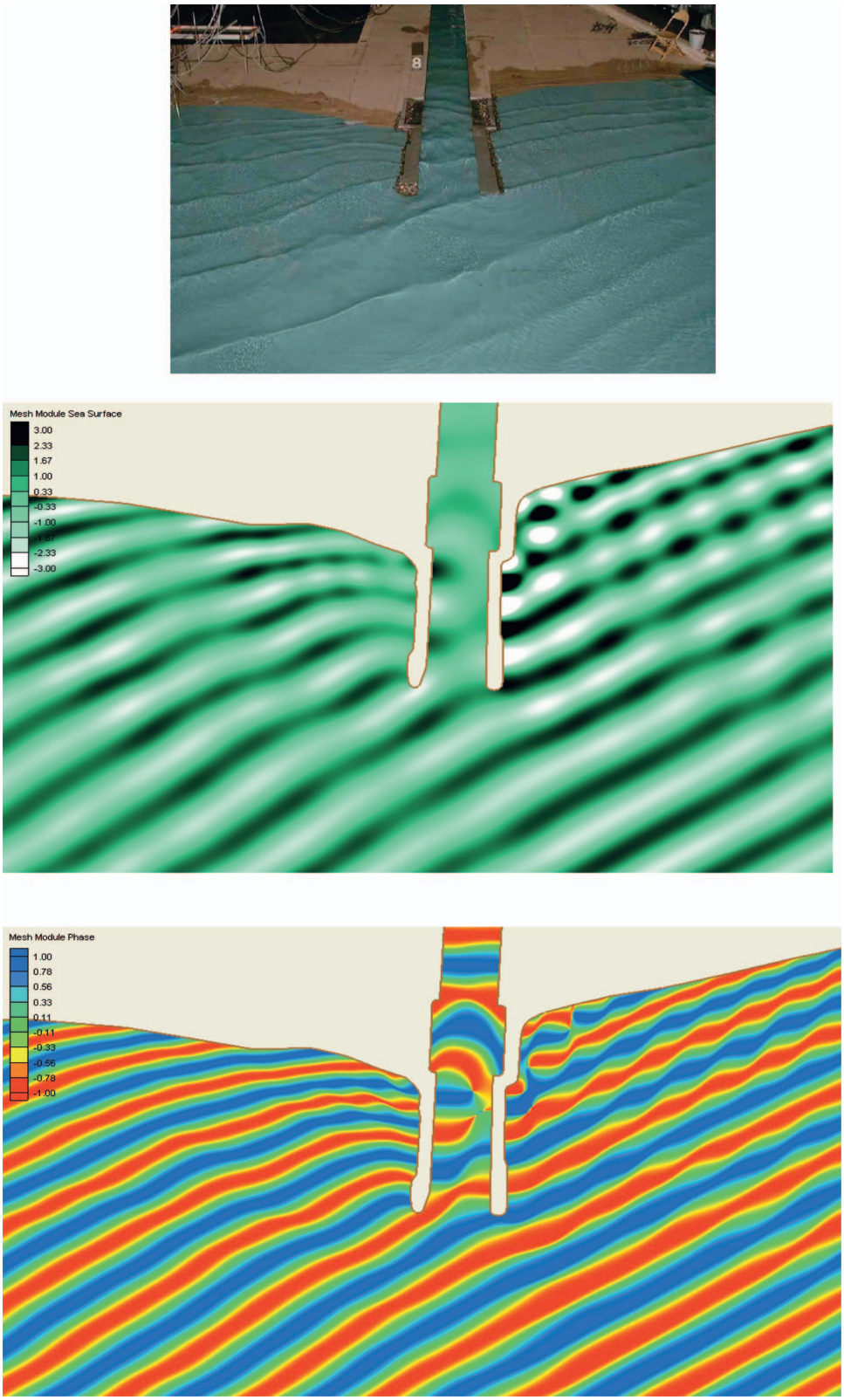

Fig. 17. (Color) Hydraulic and numerical model sea surface snapshot (top two panels) and numerical model phase diagram (bottom panel) for oblique wave incidence

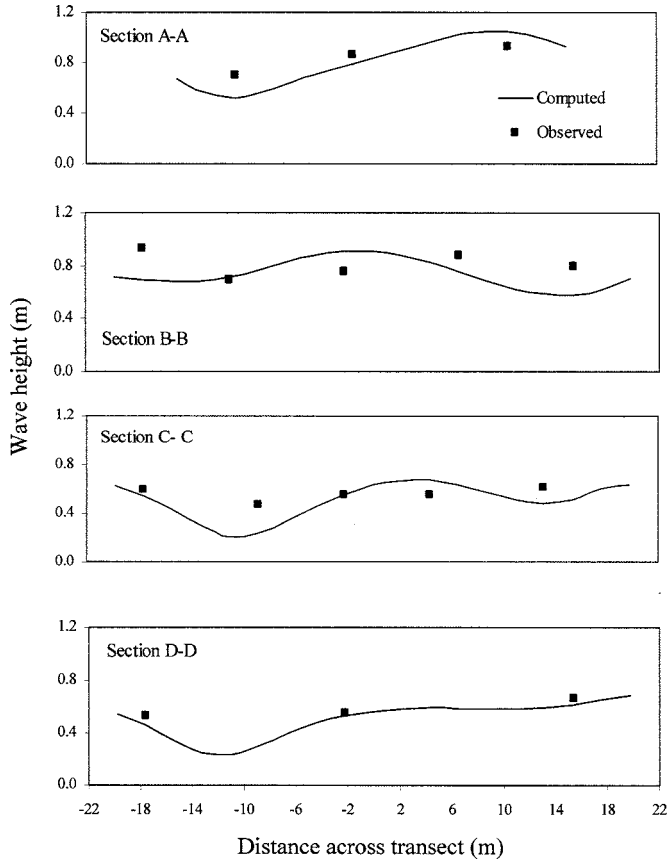

Fig. 18. Wave height comparison, H_i=1 m, T=5 s

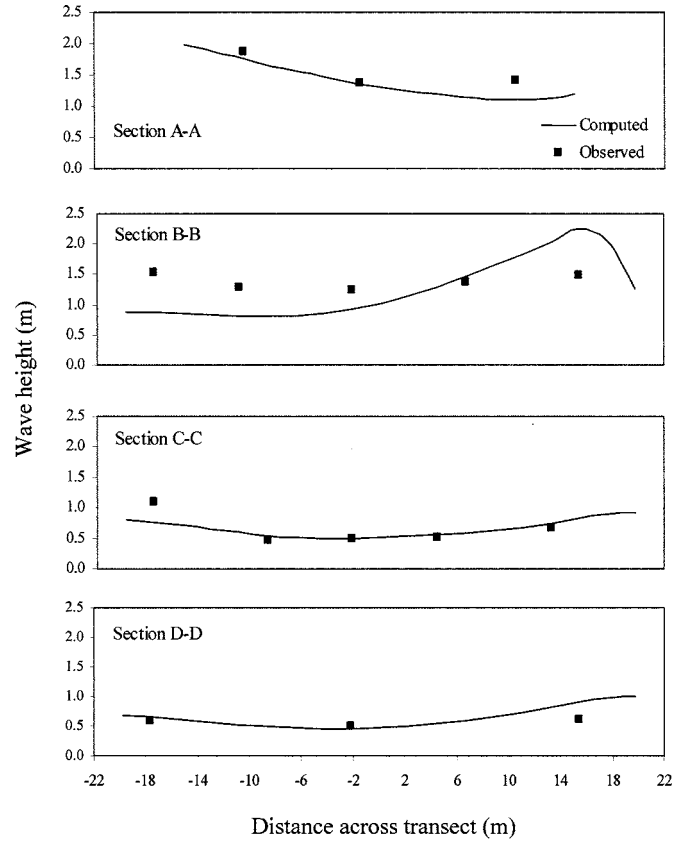

Fig. 19. Wave height comparison, H_i=2 m, T=7 s

angles of 0° and 45°, respectively. (For case (c), no photographs are available; however, quantitative results are presented later.) In general, the both modeled wave patterns are similar. A comparison of model results with gauge data along the 4 transects for cases (a) and (c), shown in Figs. 18 and 19 suggests that the numerical model captures the salient features of the observed wave patterns reasonably well. In general, the data show wave height attenuation as one goes down the channel; the reduction in the vicinity of transects CC and DD is approximately 80% and 50% in case (a), and 75% and 30% in case (c). There are some discrepancies, which can perhaps be attributed to the following factors: The overall pattern of the wave field seen in Figs. 16 and 17 is fairly complex in the channel and near the structures, suggesting that more gauge measurements may be needed to properly represent the wave field. Also the incident spectrum was unknown, as was the exact location of the gauges. The properties of the rubble mound structure such as the exact width, porosity, etc. were also unknown and our choice of the parameters may influence the comparison.

Thompson et al. (2004) have noted the absence of guidelines for designing pocket absorbers and have noted that the designer has several options. Here we examine, for case (a), the effects of eliminating one pocket and of staggering the pockets on either side wall (configurations B and E in Fig. 1). The results (Fig. 20) may be compared with those in Fig. 15 (bottom panel) where two (nearly) symmetric pocket absorbers are included. The wave heights in the entrance channel seem to experience much greater reflection when the two pocket absorbers are staggered (Fig. 20, bottom panel), and surprisingly, the wave heights in the channel resulting from the use of just one pocket are somewhat lower than when two pockets are used.

Concluding Remarks

The effect of rubble mound structures has hitherto been included in models based on the parabolic approximation of the mild-slope wave equation (Melo and Guza 1991a,b) or on the 3D Laplace equation (Sulisz 2005). Relative to the elliptic mild-slope wave equation that is widely used in harbor applications, these models have limitations rooted in their computational attributes or in their ability to simulate angular scattering. We have therefore explored the incorporation of the related dissipation mechanism in the 2D elliptic equation. Although the dissipation formulation that is invoked is essentially the same as in earlier models (based on the Lorentz principle), the iterative treatment of the nonlinearity is fundamentally different.

The resulting model was applied to an idealized pocket absorber (studied by Sulisz [2005]) and to straight and curved channels bounded by rubble mound (studied by Melo and Guza [1991a,b] and by Melo and Gobi [1999] as an approximate version of the Mission Bay entrance channel). The model was also applied to a pocket absorber patterned after the Pentwater Harbor entrance (Thompson et al. 2006). For the idealized pocket absorber, the solutions of the present 2D elliptic model match the 3D solutions of Sulisz (2005) quite well. This test not only provides model validation against a more complete (3D) solution but also shows that the pocket absorbers can create regions of high wave heights on the up-wave side; these reflected waves can potentially be hazardous to small craft operation. In the case of the

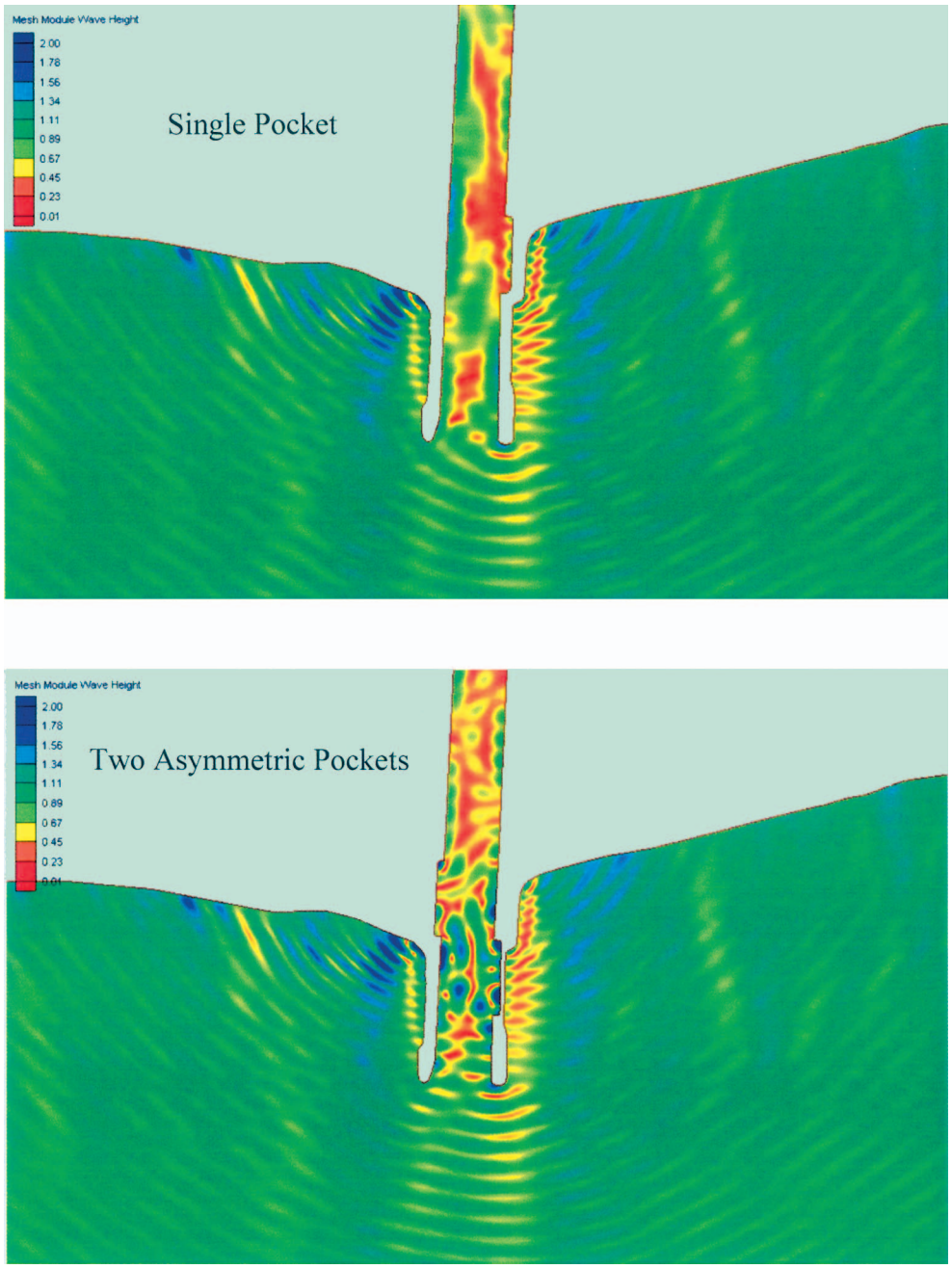

Fig. 20. (Color) Modeled wave heights for alternative entrance channel configurations

straight channel, the results of the parabolic approximation were similar to the present results. A good match was also seen in the case of the curved channel when the simulations involved no dissipation; however, when dissipation was modeled, the results of the full elliptic model deviated from those of the parabolic approximation, suggesting that dissipation can enhance the angular scattering of waves and be a further impediment to the parabolic models. The elliptic model results also captured, in a qualitative sense, most of the features seen in photographs of hydraulic model simulations of the Pentwater Bay entrance channel. Quantitatively, too, the attenuation measured along transects downwave of the pocket absorber was largely captured. For the Pentwater Bay entrance channel, alternative arrangements for the pocket absorbers were considered as an illustration. The results showed that for the incident wave condition examined, the configuration with one absorber was the most effective in reducing the wave heights.

The results summarized above suggest that incorporating dissipative effects as described here can be an effective method of extending the practical utility of existing 2D elliptic harbor wave simulation models, to address, for example, the need for design tools as stated by Thompson et al. (2004) in the context of pocket wave absorbers in the Great Lakes region.

Acknowledgments

This research was supported by the Coastal Inlets Research Program (CIRP), U.S. Army Engineer R&D Center (for ZD).

Permission was granted by Headquarters, U.S. Army Corps of Engineers, to publish this information.

References

Booij, N. (1981). "Gravity waves on water with nonuniform depth and current." Ph.D. thesis, Technical Univ. of Delft, The Netherlands.

Bova, S. W., Breshears, C. P., Cuicchi, C., Demirbilek, Z., and Gabb, H. A. (2000). "Dual level parallel analysis of harbor wave response using MPI and OpenMPI." *Int. J. High Perform. Comput. Appl.*, 14(1), 49–64.

Chandrasekera, C. N., and Cheung, K. F. (1997). "Extended linear refraction-diffraction model." *J. Waterway, Port, Coastal, Ocean Eng.*, 123(5), 280–286.

Chen, W., Panchang, V. G., and Demirbilek, Z. (2005). "On the modeling of wave-current interaction using the elliptic mild-slope wave equation." *Ocean Eng.*, v32, 2135–2164.

Dalrymple, R. A., Kirby, J. T., and Hwang, P. A. (1984). "Wave diffraction due to areas of energy dissipation." *J. Waterway, Port, Coastal, Ocean Eng.*, 110(1), 67–79.

Demirbilek, Z., and Panchang, V. G. (1998). "CGWAVE: A coastal surface water wave model of the mild slope equation." *Technical Rep. CHL-98-26*, U.S. Army Corps of Engineers Waterways Expert Station, Vicksburg, Miss.

Kostense, J. K., Dingemans, M. W., and Bosch, P. van den. (1988). "Wave-current interaction in harbours." *Proc. 21st Int. Conf., Coastal Eng.*, Vol. 1, ASCE, New York, 32-46.

Li, B. (1994). "A generalized conjugate gradient model for the mild slope equation." *Coastal Eng.*, 23, 215–225.

Li, D., Panchang, V. G., Tang, Z., Demirbilek, Z., and Ramsden, J. (2005). "Evaluation of an approximate method for incorporating floating docks in two-dimensional harbor wave prediction models." *Can. J. Civ. Eng.*, 32, 1082–1092.

Mattioli, F. (1996). "Dynamic response of the Lido channel to wave motion in the presence of movable barriers." *Il Nuovo Cimento C*, 19, 177–194.

Melo, E., and Gobbi, M. F. (1998). "Wave propagation in circular jettied channels." *J. Waterway, Port, Coastal, Ocean Eng.*, 124(1), 7–15.

Melo, E., and Guza, R. T. (1990). *Wave propagation in a jettied channel entrance*, SIO Reference Series 90-1, Scripps Institution of Oceanography, La Jolla, Calif.

Melo, E., and Guza, R. T. (1991a). "Wave propagation in jettied entrance channels I: Models." *J. Waterway, Port, Coastal, Ocean Eng.*, 117(5), 471–492.

Melo, E., and Guza, R. T. (1991b). "Wave propagation in jettied entrance channels II: Observations." *J. Waterway, Port, Coastal, Ocean Eng.*, 117(5), 493–510.

Okihiro, M., and Guza, R. T. (1996). Observations of seiche forcing and amplification in three small harbors. *J. Waterway, Port, Coastal, Ocean Eng.*, 122(5), 232–238.

Panchang, V., Chen, W., Xu, B., Schlenker, K., Demirbilek, Z., and Okihiro, M. (2000). "Exterior bathymetric effects in elliptic harbor wave models." *J. Waterway, Port, Coastal, Ocean Eng.*, 126(2), 71–78.

Panchang, V. G., and Demirbilek, Z. (2001). "Simulation of waves in harbors using two-dimensional elliptic equation models." *Adv. in Coastal and Ocean Engrg.*, World Scientific, 7, 125–162.

Panchang, V. G., Ge, W., Cushman-Roisin, B., and Pearce, B. R. (1991). "Solution to the mild-slope wave problem by iteration." *Appl. Ocean. Res.*, 13(4), 187–199.

Sulisz, W. (2005). "Wave propagation in channel with side porous caves." *J. Waterway, Port, Coastal, Ocean Eng.*, 131(4), 162–170.

Tang, Y., Ouellet, Y., and Ropars, Y. (1999). "Finite element modelling of wave conditions inside sainte-Therese-de-Gaspe Harbour, Quebec." *Proc. Canadian Coastal Conf.*, 737–748.

Thompson, E. F., et al. (2006). "Monitoring of entrance channel navigation improvements at Pentwater, Michigan, and design guidance for pocket wave absorbers." *Technical Rep. TR-06-3*, U.S. Army Corps of Engineers Waterways Expert Station, Vicksburg, Miss.

Thompson, E. F., Bottin, R. R., and Selegean, J. P. (2004). "Effectiveness of pocket wave absorbers in vertical-wall, coastal entrance structures." *Technical Rep. ERDC/CHL CHETN-III-69*, U.S. Army Corps of Engineers Waterways Expert Station, Vicksburg, Miss.

Thompson, E. F., Bottin, R. R., and Shak, A. T. (2002). *Monitoring of entrance channel navigation improvements at Morro Bay Harbor, Morro Bay, California*, USACOE, ERDC, TR-02-18, Vicksburg, Miss.

Thompson, E. F., and Demirbilek, Z. (2002). *Wave climate and wave response, 2025 Plan, Kahului Harbor, Hawaii*, USACOE, ERDC, TR-02-21, Vicksburg, Miss.

Tsay, T. K., Zhu, W., and Liu, P. L. F. (1989). "A finite-element model for wave refraction, diffraction, reflection, and dissipation." *Appl. Ocean. Res.*, 11, 33–38.

Zhao, L., Panchang, V. G., Chen, W., Demirbilek, Z., and Chhabbra, N. (2001). "Simulation of breaking effects in a two-dimensional harbor wave prediction model." *Coastal Eng.*, 42(4), 359–373.

Zubier, K., Panchang, V. G., and Demirbilek, Z. (2003). "Simulation of waves at Duck (North Carolina) using two numerical models," *Coastal Engineering Journal*, 45(3), 439–469.